

Laser-induced periodic surface structure. I. Theory

J. E. Sipe, Jeff F. Young, J. S. Preston, and H. M. van Driel

Department of Physics and Erindale College, University of Toronto, Toronto, Ontario M5S 1A7, Canada

(Received 20 April 1982)

We develop a theory for laser-induced periodic surface structure by associating each Fourier component of induced structure with the corresponding Fourier component of inhomogeneous energy deposition just beneath the surface. We assume that surface roughness, confined to a region of height much less than the wavelength of light, is responsible for the symmetry breaking leading to this inhomogeneous deposition; we find strong peaks in this deposition in Fourier space, which leads to predictions of induced fringe patterns with spacing and orientation dependent on the angle of incidence and polarization of the damaging beam. The nature of the generated electromagnetic field structures and their relation to the simple "surface-scattered wave" model for periodic surface damage are discussed. Our calculation, which is for arbitrary angle of incidence and polarization, applies a new approach to the electrodynamics of randomly rough surfaces, introducing a variational principle to deal with the longitudinal fields responsible for local field, or "depolarization," corrections. For a p -polarized damaging beam our results depend on shape and filling factors of the surface roughness, but for s -polarized light they are essentially independent of these generally unknown parameters; thus an unambiguous comparison of our theory with experiment is possible.

I. INTRODUCTION

Many researchers studying the interaction of intense laser beams and solids are familiar with the striking periodic damage patterns that can be produced on various surfaces when the power of the beam is at or near the damage threshold. Grating-like damage patterns, resulting from illumination with *single beams* of intense laser radiation, have been observed at the surfaces of targets made of various intrinsic and extrinsic semiconductors,¹⁻⁷ metals,⁸⁻¹¹ and dielectrics,¹² using cw to picosecond laser sources between 0.53 and 10.6 μm . Explanations of this periodic damage have been given in terms of properties of the laser beam,¹ frozen surface acoustic waves,⁴ and plasmon condensation.^{10,13} However, most of the damage patterns are remarkably similar and independent of material properties. When the beam is normally incident the damage appears in the form of parallel, periodic lines of separation λ , the wavelength of the incident light; these lines, or "fringes," run perpendicular to the polarization of the incident field. If a scratch is purposely placed on the surface prior to irradiation and if the angle of incidence θ is varied, two sets of fringes on the sides of the scratch are found,⁵ with spacings of $\lambda/(1 \pm \sin\theta)$.

The observation of fringes created near a scratch indicates that, at least for a wide class of materials, surface roughness is responsible for the symmetry

breaking necessary to produce periodic surface damage. The occurrence of the fringes has been attributed to the interference of the incident beam with a "surface-scattered wave" originating at the scratch.^{2,5} Although this picture of the damage formation is appealing, it is not physically consistent for a number of reasons: Since the damage patterns are presumably produced by the absorption of energy within the material, it is not clear why the surface-scattered wave responsible should propagate with a wavelength of λ as opposed to λ/n , where n is the refractive index of the material. Further, at normal-incidence excitation, the scattered wave would have to be longitudinally polarized; such waves do not satisfy the Maxwell equations. In fact, plane waves of *any* polarization, propagating parallel to an interface, do not satisfy the Maxwell equations. Temple and Soileau¹² have recently argued that nonradiative, short-range fields associated with surface defects can perhaps account for the surface-scattered wave. Approximating the dipole field from a defect as only a retarded static-zone field, and completely neglecting the presence of the surface on the generated field, they have extended calculations by Bloembergen¹⁴ of enhanced fields *within* defects to try to understand the development of fringes external to isolated defects. In addition, they have reported that at normal incidence the fringe spacing associated with 10.6- μm -radiation damage in NaCl is λ/n .

Recently we have reported a new set of fringes which are produced at the surface of nominally smooth Ge samples by laser irradiation at $1.06 \mu\text{m}$ and have a spacing of $\lambda/\cos\theta$.^{6,15} These fringes, which run *parallel* to the polarization of the incident light, are produced only with *p*-polarized light at large angles of incidence; in fact, $\lambda/(1+\sin\theta)$, $\lambda/(1-\sin\theta)$, and $\lambda/\cos\theta$ fringes can under some conditions be produced simultaneously. Further, we have shown that a previously unappreciated richness in the damage structure can be studied by observing the intensity $I(\vec{\kappa})$ of the diffraction pattern produced by illuminating the damaged surface with a weak probe beam; here $\vec{\kappa}$ is the wave vector parallel to the surface. The above-mentioned $\lambda/\cos\theta$ fringes appear as particularly bright spots in the diffraction pattern, but in general there is damage produced over a wide range of $\vec{\kappa}$'s. After a certain amount of irradiation this diffraction pattern stabilizes; the final $I(\vec{\kappa})$ is remarkably independent of the specific surface inhomogeneities that are initially present.

These results suggest that some insight into the damage process can be gained by studying the damage in $\vec{\kappa}$ space, rather than by watching the development of local damage around isolated defects on the surface. A first attempt at the calculation of the intensity function $I(\vec{\kappa})$, avoiding the difficulties of the heuristic "surface-scattered wave" picture, is the subject of this paper.

To do this we adopt a very simple picture of the way in which damage occurs at the surface (see Fig. 1). A laser beam, idealized as an infinite plane wave, is incident with a wave vector of magnitude $\tilde{\omega} = 2\pi/\lambda$ on a rough surface; the wave-vector component parallel to the surface is designated by $\vec{\kappa}_i$, $|\vec{\kappa}_i| = \tilde{\omega} \sin\theta$. The roughness is assumed to be confined in a "selvedge region" between $z=0$ and $z=l$, where $l/\lambda \ll 1$. If there were no surface roughness present, only the usual refracted beam (with wave vector $\vec{\kappa}_i$ parallel to the surface) would appear in the bulk; owing to a Fourier component of surface roughness at $\vec{\kappa}$, however, "scattered" fields appear

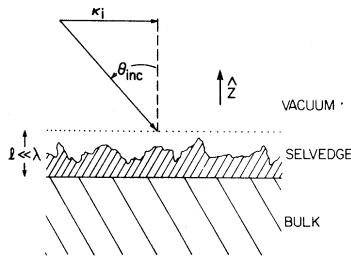


FIG. 1. The geometry of light incident on a rough surface.

in the bulk at $\vec{\kappa}_{\pm} = \vec{\kappa}_i \pm \vec{\kappa}$. These interfere with the refracted beam to lead to inhomogeneous absorption at $z=0$ — with a wave vector $\vec{\kappa}$ parallel to the surface, and with a magnitude $\eta(\vec{\kappa}; \vec{\kappa}_i) |b(\vec{\kappa})|$; $b(\vec{\kappa})$ is a measure of the amplitude of the surface roughness at $\vec{\kappa}$, and $\eta(\vec{\kappa}; \vec{\kappa}_i)$ is a response function describing the efficacy with which surface roughness at $\vec{\kappa}$ leads to inhomogeneous absorption just below the selvedge for a given incident field. Neglecting all feedback processes that are undoubtedly important in the detailed development of the damage, and considering only the region of bulk material just below the surface roughness, we simply assume that the damage occurs first where this inhomogeneous absorption is largest, leading to a prediction

$$I(\vec{\kappa}) \propto \eta(\vec{\kappa}; \vec{\kappa}_i) |b(\vec{\kappa})|. \quad (1.1)$$

Perhaps the most interesting of our results is that $\eta(\vec{\kappa}; \vec{\kappa}_i)$ exhibits very sharp peaks and thus, for a nominally smooth surface, we can understand the independence of $I(\vec{\kappa})$ on the details of the more-or-less random roughness present; those details are responsible only for determining the exact form of the more smoothly varying $b(\vec{\kappa})$.

The above-mentioned sharp peaks occur at values of $\vec{\kappa}$ that satisfy

$$|\vec{\kappa}_i \pm \vec{\kappa}| = \tilde{\omega} \quad (1.2a)$$

or

$$|\vec{\kappa}_i \pm \vec{\kappa}| = \tilde{\omega} n. \quad (1.2b)$$

These conditions include, as special cases, all the fringe spacings and directions mentioned above. We show that Eqs. (1.2) correspond to the generation of nonradiative field structures which we call "radiation remnants"; in terms of these we can construct a more satisfactory physical picture of the electromagnetic aspect of the damage than that provided by the phenomenological "surface-scattered wave" concept. Further, we find that condition (1.2a) leads to the peaks important in metals and in semiconductors and dielectrics with large refractive indices; condition (1.2b) can apply for materials with $n \simeq 1$. This is in general agreement with the experimental results.¹⁻¹²

In addition, we find that not all the $\vec{\kappa}$ satisfying the appropriate condition (1.2) exhibit a peak; the specific values of $\vec{\kappa}$ that do depend strongly on the angle of incidence and polarization of the incident beam. This dependence appears because of the variation with angle of incidence and polarization of the relative amplitudes of the induced polarization fields, in the selvedge, that are parallel and perpendicular to the surface. To predict these amplitudes correctly we have extended the usual perturbation treatments of the electromagnetic properties of

rough surfaces.¹⁶⁻²⁰ In those treatments the shape-dependent "local-field corrections," which are crucially important for materials of large dielectric constant (in Ge, $\epsilon \simeq 16$ at $1.06 \mu\text{m}$), would require the summation of an infinite series for their correct inclusion. Instead we calculate the polarization field components in the selvedge by first separating the longitudinal and transverse components of the electromagnetic field. The latter, in the limit $l \ll \lambda$, can be safely treated by a perturbation series which then describes "multiple scattering"; the former, which is short ranged and responsible for the local-field corrections, is treated by constructing a variational principle and finding an approximate solution for the polarization field. Thus we take into account the local-field effects which are so important here and in other surface optics problems such as surface-enhanced Raman scattering²¹ (SERS) and which are usually described by phenomenological models of rough surfaces as collections of spheres or ellipsoids on a smooth surface²²; our approach is more fundamental and more general.

We begin with an integral formulation of the electromagnetic problem, which we present in Sec. II; the advantage of an integral formulation in other problems in electromagnetic theory is well known.²³ In Sec. III we discuss the "radiation remnant" field structures. Although the importance of nonradiative fields in this problem has been suggested by other workers,^{6,12,15} this is the first time these field structures have been identified, studied, and discussed in detail. In Sec. IV we decompose the electromagnetic field in the selvedge into longitudinal and transverse parts, introduce the variational principle, and present an approximate solution for the polarization in the selvedge. This is used in Sec. V to calculate $\eta(\vec{\kappa}; \vec{\kappa}_i)$, the central result of this work. The main features of this function are noted; detailed comparison of theory with experiment appears in the following paper of this series.²⁴

II. THE SELVEDGE POLARIZATION EQUATIONS

We begin by developing an integral equation for the polarization in the selvedge region of Fig. 1. Neglecting magnetic effects, the electromagnetic field generated by the polarization $\vec{P}(\vec{r}, t)$ in the medium satisfies the Maxwell equations

$$\begin{aligned} \vec{\nabla} \cdot \vec{E}(\vec{r}) &= -4\pi \vec{\nabla} \cdot \vec{P}(\vec{r}), \quad \vec{\nabla} \cdot \vec{B}(\vec{r}) = 0, \\ \vec{\nabla} \times \vec{B}(\vec{r}) + i\tilde{\omega} \vec{E}(\vec{r}) &= -4\pi i \tilde{\omega} \vec{P}(\vec{r}), \end{aligned} \quad (2.1)$$

$$\vec{\nabla} \times \vec{E}(\vec{r}) - i\tilde{\omega} \vec{B}(\vec{r}) = 0,$$

where we deal with stationary fields,

$$f(\vec{r}, t) = \text{Re}[f(\vec{r})e^{-i\omega t}], \quad (2.2)$$

for all fields $f(\vec{r}, t)$, and we have put $\tilde{\omega} = \omega/c$. Fourier decomposing in the xy plane

$$f(\vec{r}) = \int \frac{d\vec{\kappa}}{(2\pi)^2} f(\vec{\kappa}; z) e^{i\vec{\kappa} \cdot \vec{r}}, \quad (2.3)$$

where $\vec{\kappa} = (\kappa_x, \kappa_y)$ and $\vec{r} = (x, y)$, the solution of Eqs. (2.1) for \vec{E} , with the particular part satisfying the outgoing wave condition at $z \rightarrow \pm \infty$, is^{25,26}

$$\vec{E}(\vec{\kappa}; z) = \vec{E}_0(\vec{\kappa}; z) + \int \vec{G}(z - z') \cdot \vec{P}(\vec{\kappa}; z') dz', \quad (2.4)$$

where the $\vec{\kappa}$ dependence of \vec{G} and \vec{G}_0

$$\begin{aligned} \vec{G}(z - z') &= \vec{G}_0(z - z') - 4\pi \hat{z} \hat{z} \delta(z - z'), \\ \vec{G}_0(z - z') &= \vec{g}_+(\vec{\kappa}) \Theta(z - z') e^{i\omega_0(z - z')} \\ &\quad + \vec{g}_-(\vec{\kappa}) \Theta(z' - z) e^{i\omega_0(z' - z)}, \end{aligned} \quad (2.5)$$

is kept implicit. We have set

$$\vec{g}_{\pm}(\vec{\kappa}) = 2\pi i \omega_0^{-1} \tilde{\omega}^2 (\hat{s} \hat{s} + \hat{p}_{0\pm} \hat{p}_{0\pm}), \quad (2.6)$$

where

$$\begin{aligned} \hat{s} &= \hat{\kappa} \times \hat{z}, \\ \omega_0 &= (\tilde{\omega}^2 - \kappa^2)^{1/2}, \quad \text{Re} \omega_0, \text{Im} \omega_0 \geq 0, \\ \hat{p}_{0\pm} &= \tilde{\omega}^{-1} (\kappa \hat{z} \mp \omega_0 \hat{\kappa}), \end{aligned}$$

and $\Theta(z)$ is the unit step function, $\Theta(z) = 1, 0$ as $z > 0, z < 0$. The dyadic Green function (2.5) explicitly identifies the s - and p -polarized components of the (propagating or evanescent) wave generated at each $\vec{\kappa}$ by the polarization.²⁷ The field $\vec{E}_0(\vec{\kappa}; z)$ is the Fourier transform (2.3) of the appropriate homogeneous solution of Eqs. (2.1); for a beam incident from $z = +\infty$, it takes the form

$$\vec{E}_0(\vec{\kappa}; z) = \vec{E}_0(\vec{\kappa}) e^{-i\omega_0 z}, \quad (2.7)$$

where $\vec{E}_0(\vec{\kappa})$ can have an \hat{s} and a \hat{p}_{0-} component, corresponding to s - and p -polarized waves, respectively.

Consider now points in the bulk region ($z < 0$). Using Eqs. (2.4) and (2.7), we may write

$$\begin{aligned} \vec{E}(\vec{\kappa}; z) &= \vec{E}'_0(\vec{\kappa}) e^{-i\omega_0 z} \\ &\quad + \int_{z'=-\infty}^0 \vec{G}(z - z') \cdot \vec{P}(\vec{\kappa}; z') dz', \end{aligned} \quad (2.8)$$

where

$$\begin{aligned} \vec{E}'_0(\vec{\kappa}) &= \vec{E}_0(\vec{\kappa}) + \vec{g}'_-(\vec{\kappa}) \cdot \vec{Q}(\vec{\kappa}), \\ \vec{Q}(\vec{\kappa}) &= \int_{z'=0}^l e^{i\omega_0 z'} \vec{P}(\vec{\kappa}; z') dz'. \end{aligned} \quad (2.9)$$

From Eq. (2.8) it is clear that the material in the bulk sees an effective incident field $\vec{E}'_0(\vec{\kappa})$, including the field generated by sources in the selvedge region. If the bulk is characterized by a susceptibility χ ,

$$\vec{P}(\vec{r}) = \chi \vec{E}(\vec{r}), \quad (2.10)$$

the response of the bulk material to the effective incident field $\vec{E}_0(\vec{\kappa})$ [the solution of Eq. (2.8)] has the well-known form

$$\vec{E}(\vec{\kappa}; z) = e^{-i\omega z} \vec{t}(\vec{\kappa}) \cdot \vec{E}_0(\vec{\kappa}) \quad (z < 0), \quad (2.11)$$

where

$$\vec{t}(\vec{\kappa}) = \hat{s} \hat{s} t_s + \hat{p}_- \hat{p}_0 - t_p. \quad (2.12)$$

Here

$$\begin{aligned} \hat{p}_- &= (\tilde{\omega} n)^{-1} (\kappa \hat{z} + w \hat{\kappa}), \\ w &= (\tilde{\omega}^2 \epsilon - \kappa^2)^{1/2}, \end{aligned} \quad (2.13)$$

where $\epsilon = 1 + 4\pi\chi$ is the dielectric constant of the bulk; \hat{p}_- specifies the polarization of a downward propagating (or evanescent) p -polarized wave in the bulk. In Eq. (2.13), $\text{Im}w \geq 0$, and $\text{Re}w \geq 0$ if $\text{Im}w = 0$; $n = \epsilon^{1/2}$, subject to the same conditions. The matrix $\vec{t}(\vec{\kappa})$ involves the Fresnel coefficients for s - and p -polarized light,

$$\begin{aligned} t_s &= 2w_0(w_0 + w)^{-1}, \\ t_p &= 2w_0 n(w_0 \epsilon + w)^{-1}, \end{aligned} \quad (2.14)$$

respectively. Equation (2.11) will be useful later, but we presently need the electric field (2.4) in the selvedge region. Separating the contributions to the integral in Eq. (2.4) into the regions $-\infty < z' < 0$ and $0 < z' < l$, we note that the former is just the field due to polarizations in the bulk; since the bulk is subject to an effective incident field (2.9), the required contribution is just

$$e^{i\omega_0 z} \vec{r}(\vec{\kappa}) \cdot \vec{E}'_0(\vec{\kappa}), \quad (2.15)$$

where

$$\vec{r}(\vec{\kappa}) = r_s \hat{s} \hat{s} + r_p \hat{p}_0 + \hat{p}_0 - \quad (2.16)$$

involves the Fresnel reflection coefficients for s - and p -polarized light,

$$\begin{aligned} r_s &= (w_0 - w)(w_0 + w)^{-1}, \\ r_p &= (w_0 \epsilon - w)(w_0 \epsilon + w)^{-1}, \end{aligned} \quad (2.17)$$

respectively. Thus, for points $0 < z < l$, Eq. (2.4) takes the form

$$\begin{aligned} \vec{E}(\vec{\kappa}; z) &= \vec{E}_0(\vec{\kappa}) e^{-i\omega_0 z} + \vec{r}(\vec{\kappa}) \cdot \vec{E}'_0(\vec{\kappa}) e^{i\omega_0 z} \\ &+ \int_{z'=0}^l \vec{G}(z-z') \cdot \vec{P}(\vec{\kappa}; z') dz', \end{aligned} \quad (2.18)$$

or using Eqs. (2.8) and (2.9),

$$\begin{aligned} \vec{E}(\vec{\kappa}; z) &= \vec{E}_i(\vec{\kappa}; z) + \int_{z'=0}^l \vec{G}(z-z') \cdot \vec{P}(\vec{\kappa}; z') dz' \\ &+ \int_{z'=0}^l \vec{S}(z+z') \cdot \vec{P}(\vec{\kappa}; z') dz', \end{aligned} \quad (2.19)$$

where

$$\begin{aligned} \vec{E}_i(\vec{\kappa}; z) &= \vec{E}_0(\vec{\kappa}) e^{-i\omega_0 z} + \vec{r}(\vec{\kappa}) \cdot \vec{E}_0(\vec{\kappa}) e^{i\omega_0 z}, \\ \vec{S}(z+z') &= 2\pi i \omega_0^{-1} \tilde{\omega}^2 (r_s \hat{s} \hat{s} + r_p \hat{p}_0 + \hat{p}_0 -) \\ &\times e^{i\omega_0(z+z')}. \end{aligned} \quad (2.20)$$

The first term on the right-hand side of Eq. (2.19) is the field that would be present in the selvedge region if there were no polarization in the selvedge; the second term is the field in the selvedge region due to the polarization in the selvedge; the third term is the field there due to polarization in the bulk induced by the polarization in the selvedge.

We now introduce a constitutive relation for the polarization in the selvedge; we take the simple form

$$\vec{P}(\vec{r}) = \chi(\vec{r}) \vec{E}(\vec{r}) \quad (0 < z < l), \quad (2.21)$$

where

$$\chi(\vec{r}) = \chi b(\vec{r}), \quad (2.22)$$

and $b(\vec{r}) = 0, 1$, respectively, in the "unfilled" part of the selvedge and in the region filled by material. We shall here assume for simplicity that the susceptibility of the material in the selvedge [χ of Eq. (2.22)] is the same as that of the bulk [Eq. (2.20)]; however, we note that the generalization of the equations in this and following sections to treat selvedge material with a different susceptibility is straightforward.

Equations (2.19) and (2.21), using Eq. (2.22), completely determine the polarization in the selvedge and, within the approximation of Eq. (2.21), do so exactly. Note that they involve only the polarization field at points *in the selvedge itself*; the effect of the polarization in the bulk enters through the Fresnel coefficients appearing in Eqs. (2.20). Once the polarization in the selvedge is determined from Eqs. (2.19) and (2.21), the field in the bulk follows from Eqs. (2.9) and (2.11); the field in the vacuum above is simply given by

$$\begin{aligned} \vec{E}(\vec{\kappa}; z) &= e^{i\omega_0 z} \vec{r}(\vec{\kappa}) \cdot \vec{E}'_0(\vec{\kappa}) \\ &+ \int_0^l \vec{G}(z-z') \cdot \vec{P}(\vec{\kappa}; z') dz' \quad (z > l), \end{aligned} \quad (2.23)$$

the first term being the field from polarizations in the bulk and the second from the selvedge polarization [cf. Eqs. (2.4), (2.5), and (2.15)].

III. RADIATION REMNANTS

Before considering a self-consistent solution of the selvedge polarization Eqs. (2.19) and (2.21), we look first at the electric field generated by a *specified, imposed* $\vec{Q}(\vec{\kappa})$ [Eq. (2.9)]. This is important because

the field generated by a fixed $|\vec{Q}|$ is, as a function of κ , not analytic; there are discontinuities in the first derivative of the function at certain critical points and these "kinks" are crucial in the development of fringes, as we will argue in Sec. V. The presence of these discontinuities and their physical interpretation are the subjects of this section. To aid the discussion, we shall introduce a (complex) electromagnetic self-energy for the selvedge.

Consider first the general problem of an arbitrary, specified $\vec{P}(\vec{r})$ confined to a region in space; other polarizations may be present outside that region which, unlike $\vec{P}(\vec{r})$, are induced and not imposed. We define the electromagnetic self-energy of the specified polarization $\vec{P}(\vec{r})$ as

$$\Sigma \equiv -\frac{1}{4} \int \vec{P}^*(\vec{r}) \cdot \vec{E}(\vec{r}) d\vec{r}. \quad (3.1)$$

To see the meaning of the real and imaginary parts of Σ , we note that the rate at which the current due to the imposed polarization $\vec{j}(\vec{r}, t) = \dot{\vec{P}}(\vec{r}, t)$ does work on the electromagnetic field is given by

$$\begin{aligned} W &= - \int \vec{j}(\vec{r}, t) \cdot \vec{E}(\vec{r}, t) d\vec{r} \\ &= - \int \dot{\vec{P}}(\vec{r}, t) \cdot \vec{E}(\vec{r}, t) d\vec{r} \\ &= -\frac{1}{2} \text{Re} \int \dot{\vec{P}}^*(\vec{r}) \cdot \vec{E}(\vec{r}) d\vec{r} \\ &= \frac{1}{2} \omega \text{Im} \int \vec{P}^*(\vec{r}) \cdot \vec{E}(\vec{r}) d\vec{r}, \end{aligned} \quad (3.2)$$

where in the third and fourth expressions in Eq. (3.2) we have averaged over a period [cf. Eq. (2.2)]. Thus we have

$$W = -2\omega \text{Im}\Sigma. \quad (3.3)$$

This is the steady-state rate at which work must be done on the imposed polarization to maintain it; in general, some of the energy is radiated away to ∞ while some is absorbed by the induced polarization mentioned above.

Next, consider the electromagnetic energy stored in the field distribution resulting from the imposed polarization; to calculate this, assume $\vec{P}(\vec{r}, t)$ is set up slowly and take

$$\vec{P}(\vec{r}, t) = \text{Re}[a(t)\vec{P}(\vec{r})e^{-i\omega t}] \quad (3.4)$$

$$\sigma(\vec{\kappa}) = \int_{z, z'=0}^l \vec{P}^*(\vec{\kappa}; z) \cdot [\vec{G}_0(z-z') + \vec{S}(z+z')] \cdot \vec{P}(\vec{\kappa}, z') dz dz'. \quad (3.11)$$

The second term on the right-hand side of Eq. (3.10) is a purely real contribution to $\Sigma(\vec{\kappa})$; further, it has no explicit $\vec{\kappa}$ dependence and so we shall neglect it in the following. In the limit of a selvedge of thickness much less than the wavelength and of not too large a $\vec{\kappa}$,

$$\tilde{\omega}l \ll 1, \quad \kappa l \ll 1, \quad (3.12)$$

instead of Eq. (2.2), where $a(t)=0$ at $t=-\infty$ and grows to unity at $t=0$. For a slow enough, "adiabatic" development of $\vec{P}(\vec{r}, t)$ we may assume the same form (3.4) for $\vec{E}(\vec{r}, t)$ and, using the second equation of (3.2), we find the energy required over time dt is

$$\begin{aligned} d\mathcal{E} &= (dt)\frac{1}{2}a^2(t)\omega \text{Im} \int \vec{P}^*(\vec{r}) \cdot \vec{E}(\vec{r}) d\vec{r} \\ &\quad - (dt)\frac{1}{2}a(t)\dot{a}(t)\text{Re} \int \vec{P}^*(\vec{r}) \cdot \vec{E}(\vec{r}) d\vec{r}, \end{aligned} \quad (3.5)$$

where we have averaged over a period. The first term on the right-hand side of (3.5) is the rate at which energy is radiated and possibly absorbed while $\vec{P}(\vec{r}, t)$ is being built up [cf. Eq. (3.2)]; the second term is the contribution to the energy which is stored in the field structure being developed. Integrating the second term from $t=-\infty$ to $t=0$, we find that the energy stored in the electromagnetic field, which may be either positive or negative, is

$$\begin{aligned} \mathcal{E} &= -\frac{1}{4} \text{Re} \int \vec{P}^*(\vec{r}) \cdot \vec{E}(\vec{r}) d\vec{r} \\ &= \text{Re}\Sigma. \end{aligned} \quad (3.6)$$

Combining Eqs. (3.3) and (3.6) we find

$$\Sigma = \mathcal{E} - \frac{1}{2}i\omega^{-1}W. \quad (3.7)$$

Returning now to the problem of an imposed polarization in the selvedge, we have a self-energy

$$\begin{aligned} \Sigma &= -\frac{1}{4} \int_{z=0}^l \int_{x,y=-\infty}^{+\infty} \vec{P}^*(\vec{r}) \cdot \vec{E}(\vec{r}) dx dy dz \\ &= \int \frac{d\vec{\kappa}}{(2\pi)^2} \Sigma(\vec{\kappa}), \end{aligned} \quad (3.8)$$

where

$$\Sigma(\vec{\kappa}) = -\frac{1}{4} \int_{z=0}^l \vec{P}^*(\vec{\kappa}; z) \cdot \vec{E}(\vec{\kappa}; z) dz. \quad (3.9)$$

For $\vec{E}(\vec{\kappa}; z)$ in Eq. (3.9) we use the expression (2.19) but with $\vec{E}_i(\vec{\kappa}; z)$ set equal to zero, since we here consider a specified, imposed $\vec{P}(\vec{\kappa}; z)$. We find

$$\Sigma(\vec{\kappa}) = \sigma(\vec{\kappa}) + \pi \int_{z=0}^l \vec{P}^*(\vec{\kappa}; z) \cdot \hat{z} \hat{z} \cdot \vec{P}(\vec{\kappa}; z) dz, \quad (3.10)$$

where

we have $w_0|z-z'|, w_0|z+z'| \ll 1$, and the other term simplifies considerably [cf. Eqs. (2.5) and (2.20)]. In this limit

$$\vec{Q}(\vec{\kappa}) \simeq \int_{z=0}^l \vec{P}(\vec{\kappa}; z) dz, \quad (3.13)$$

and, as can be seen by using approximations (3.12) in the equations of Sec. II, the selvedge behaves as a

“dipole sheet” placed above the bulk with a dipole moment per unit area of $\vec{Q}(\vec{\kappa})$; see also the general discussion by Sipe.²⁶ In this limit Eq. (3.11) reduces, if the polarization is in the \hat{s} direction, $\vec{P}(\vec{\kappa};z)=\hat{s}P_s(\vec{\kappa};z)$, to the form

$$\sigma(\vec{\kappa}) = -\frac{1}{2}\pi\bar{\omega} |Q_s(\vec{\kappa})|^2 f_s(\kappa), \quad (3.14)$$

while polarizations in the $\hat{\kappa}$ and \hat{z} directions lead to corresponding expressions, where

$$\begin{aligned} f_s(\kappa) &= 2i\bar{\omega}(w_0+w)^{-1}, \\ f_z(\kappa) &= 2i\kappa^2\bar{\omega}^{-1}\epsilon(w_0\epsilon+w)^{-1}, \\ f_\kappa(\kappa) &= 2i\bar{\omega}^{-1}w_0w(w_0\epsilon+w)^{-1}. \end{aligned} \quad (3.15)$$

In Sec. V we will see that response functions similar to these f 's are important in determining the position, in $\vec{\kappa}$ space, of the fringes created during laser irradiation.

The functions (3.15) are graphed in Figs. 2–4 both for the instance of an “isolated selvage” ($\epsilon=1$) and for a selvage above a material with optical properties ($\epsilon=16$) similar to germanium at 1.06 μm (see also Young *et al.*¹⁵). Consider first $f_s(\kappa)$ and $f_z(\kappa)$, which for $\epsilon=1$ are similar. For small κ we find that f is imaginary, indicating the radiation of energy to infinity; obviously, this occurs both

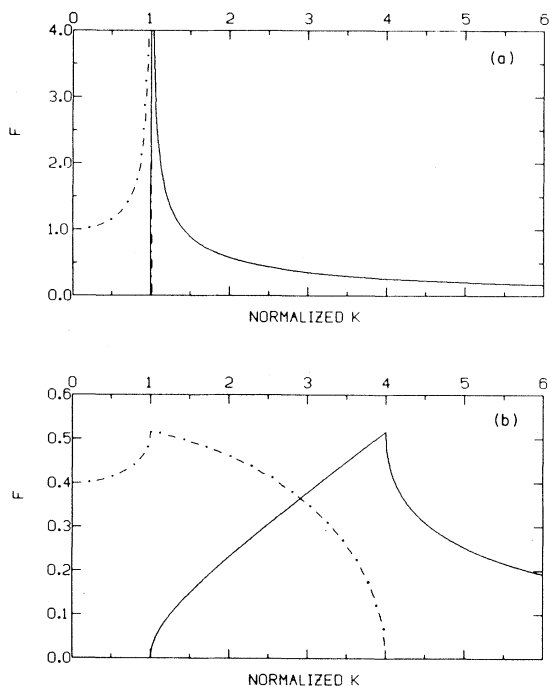


FIG. 2. (a) $\text{Re}f_s(\kappa)$ (solid line) and $\text{Im}f_s(\kappa)$ (dash-dots) for an underlying bulk with $\epsilon=1$ (vacuum). (b) $\text{Re}f_s(\kappa)$ (solid line) and $\text{Im}f_s(\kappa)$ (dash-dots) for an underlying bulk with $\epsilon=16$.

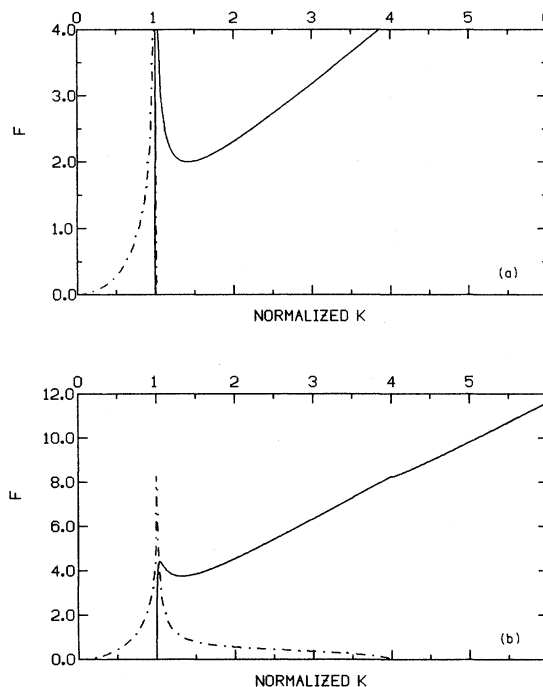


FIG. 3. (a) $\text{Re}f_z(\kappa)$ (solid line) and $\text{Im}f_z(\kappa)$ (dash-dots) for an underlying bulk with $\epsilon=1$ (vacuum). (b) $\text{Re}f_z(\kappa)$ (solid line) and $\text{Im}f_z(\kappa)$ (dash-dots) for an underlying bulk with $\epsilon=16$.

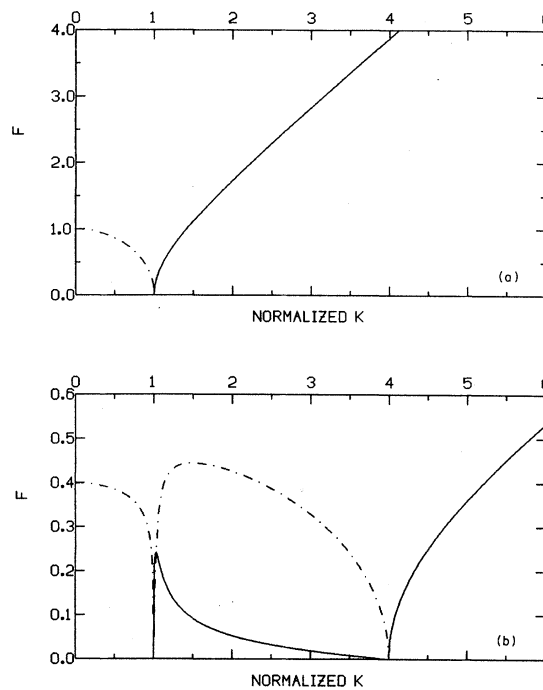


FIG. 4. (a) $-\text{Re}f_\kappa(\kappa)$ (solid line) and $\text{Im}f_\kappa(\kappa)$ (dash-dots) for an underlying bulk with $\epsilon=1$ (vacuum). (b) $-\text{Re}f_\kappa(\kappa)$ (solid line) and $\text{Im}f_\kappa(\kappa)$ (dash-dots) for an underlying bulk with $\epsilon=16$.

above and below the selvedge with respective wave vectors $\vec{k} = \kappa \hat{x} \pm |k_z| \hat{z}$ satisfying

$$\kappa^2 + k_z^2 = \tilde{\omega}^2, \quad (3.16)$$

the free radiation dispersion equation. As $\kappa \rightarrow \tilde{\omega}$ these f 's diverge, indicating the resonant, or "phase-matched," generation of radiation propagating parallel to the selvedge ($|k_z| \rightarrow 0$). For $\kappa > \tilde{\omega}$ the imaginary part of Σ must vanish, since the condition (3.16) cannot be satisfied for a real k_z ; the fields above and below the selvedge become evanescent and $W = 0$.

The situation is changed drastically for $\epsilon = 16$ [Figs. 2(b) and 3(b)]. First of all, radiation is possible up to $\kappa = n\tilde{\omega}$, since the radiation dispersion equation in the underlying bulk is given by

$$\kappa^2 + k_z^2 = (\tilde{\omega}n)^2, \quad (3.17)$$

where $n^2 = \epsilon$. Since ϵ is real and there is no absorption possible, the imaginary parts of the f 's however do strictly vanish for $\kappa > n\tilde{\omega}$, since in that regime even the fields beneath the selvedge become evanescent. Further, the divergences have disappeared, since radiation fields propagating parallel to the surface do not satisfy the Maxwell equations, regardless of the value of κ . However, "kinks" in the functions are present at both $\kappa = \tilde{\omega}$ and $\kappa = n\tilde{\omega}$, the dispersion relations for waves propagating parallel to the xy plane in an infinite vacuum and in an infinite dielectric medium, respectively.

We refer to the electromagnetic field structures signaled by these kinks in the f functions—the only nonanalytic behavior that remains in the presence of an underlying bulk with $\epsilon > 1$ —as "radiation remnants." Some insight into these fields can be obtained by considering the field generated by a source $\vec{Q}(\vec{\rho})$, which is finite in at least one direction in the xy plane. For example, consider a source

$$\vec{Q}(\vec{\rho}) = 2\pi \hat{z} \delta(\kappa_y) Q(\kappa_x), \quad (3.18)$$

where the function $Q(\vec{\rho}_x)$ is chosen so that $Q(\vec{\rho})$ is bounded in the x direction, a "ribbon" of dipoles still extending from $y = -\infty$ to $y = +\infty$. From Eq. (2.23) we find that the z component of the generated field, at $z = l +$ and within the approximations (3.12), is given by

$$E_z(x) = \tilde{\omega} \int_{-\infty}^{+\infty} f_z(\kappa) Q(\kappa) e^{i\kappa x} d\kappa. \quad (3.19)$$

In the limit $x \rightarrow +\infty$, an asymptotic expansion of Eq. (3.19) produces a leading term²⁸

$$E_z(x) \sim i\sqrt{2\pi\tilde{\omega}^3} e^{-i\pi/4} Q(\tilde{\omega}) \frac{e^{i\tilde{\omega}x}}{x^{1/2}}, \quad (3.20)$$

if $\epsilon = 1$ (isolated selvedge). The component of $Q(\kappa)$ at the κ that satisfies the dispersion relation for a ra-

diation field propagating parallel to the selvedge, $\kappa = \tilde{\omega}$, is the only component important in determining the generated $E(x)$ in the far field; the $x^{-1/2}$ factor is, of course, the characteristic signal of radiation fields in this geometry. If $\epsilon \neq 1$, however, the leading term is found to be

$$E_z(x) \sim \frac{4i\epsilon e^{i\pi/4}}{\epsilon - 1} \left[\epsilon \left[\frac{\pi\tilde{\omega}}{2} \right]^{1/2} \frac{e^{i\tilde{\omega}x}}{x^{3/2}} Q(\tilde{\omega}) - \frac{1}{\epsilon} \left[\frac{\pi n\tilde{\omega}}{2} \right]^{1/2} \frac{e^{i\tilde{\omega}nx}}{x^{3/2}} Q(\tilde{\omega}n) \right]. \quad (3.21)$$

Here the radiation fields have disappeared because of the presence of the interface; however, the kinks in $f_z(\kappa)$ lead to the important contributions in Eq. (3.19), those contributions at $\kappa = \tilde{\omega}$ and $\kappa = n\tilde{\omega}$ that would lead to radiation fields in an infinite vacuum and infinite dielectric, respectively.

The situation for an s -polarized source [Eq. (3.18) with \hat{z} replaced by $\hat{s} = -\hat{y}$] is similar; we find $E_s(x)$ is given by Eq. (3.20) if $\epsilon = 1$ and by

$$E_s(x) \sim \frac{2ie^{i\pi/4}}{(\epsilon - 1)} \left[(2\pi\tilde{\omega})^{1/2} \frac{e^{i\tilde{\omega}x}}{x^{3/2}} Q(\tilde{\omega}) - (2\pi\tilde{\omega}n)^{1/2} \frac{e^{i\tilde{\omega}nx}}{x^{3/2}} Q(\tilde{\omega}n) \right] \quad (3.22)$$

if $\epsilon \neq 1$. For a κ -polarized source the situation is interestingly different; $f_\kappa(\kappa)$ does not diverge even if $\epsilon = 1$ and in fact vanishes at $\kappa = \tilde{\omega}$, since a radiation field cannot be longitudinally polarized. In a sense, we have a "radiation remnant" even if $\epsilon = 1$, the polarization condition ruling out a radiation field, as does the interface if $\epsilon \neq 1$ for s - and z -polarized sources. This picture is borne out by the asymptotic behavior of the fields: For a $\vec{Q}(\vec{\rho})$ given by (3.18) with \hat{z} replaced by $\vec{\kappa}$ ($=\hat{x}$ here), we find

$$E_\kappa(x) \sim -i\sqrt{2\pi\tilde{\omega}} e^{i\pi/4} Q(\tilde{\omega}) \frac{e^{i\tilde{\omega}x}}{x^{3/2}} \quad \text{if } \epsilon = 1 \quad (3.23)$$

and

$$E_\kappa(x) \sim -4ie^{i\pi/4} \left[\left[\frac{\pi\tilde{\omega}}{2} \right]^{1/2} \frac{e^{i\tilde{\omega}x}}{x^{3/2}} Q(\tilde{\omega}) + \frac{1}{\epsilon} \left[\frac{\pi n\tilde{\omega}}{2} \right]^{1/2} \frac{e^{i\tilde{\omega}nx}}{x^{3/2}} Q(\tilde{\omega}n) \right] \quad \text{if } \epsilon \neq 1. \quad (3.24)$$

In both cases we have $x^{-3/2}$, nonradiative behavior (although the limits $\epsilon \rightarrow 1$ and $x \rightarrow \infty$ do not com-

mute).

We shall see in Sec. V that these “radiation remnants” are the electromagnetic field structures which, in a more exact theory, take the place of the “surface-scattered wave” concept in phenomenological theories of fringe formation. They are *not* radiation fields, as shown by Eqs. (3.20)–(3.24); thus it is not surprising that they can have either transverse (\hat{s} or \hat{z}) or longitudinal ($\hat{\kappa}$) polarization. However, they are similar to radiation fields in that they have components at $\kappa=\bar{\omega}$ and $\kappa=n\bar{\omega}$, satisfying the dispersion relations in vacuum and in the underlying medium. Further, we note that the relative amplitude of these components is dependent on n [cf., e.g., Eq. (3.21) and the relative sizes of the “kinks” in Fig. 3]. This will have important consequences in determining the spacing of fringes.

IV. THE SELVEDGE POLARIZATION

We now return to the selvedge polarization Eqs. (2.19) and (2.21) and seek a self-consistent solution. It is useful to begin by splitting the tensors \vec{G} and \vec{S} into components which lead to a longitudinal and a transverse field,

$$\begin{aligned}\vec{G} &= \vec{G}_L + \vec{G}_T, \\ \vec{S} &= \vec{S}_L + \vec{S}_T.\end{aligned}\quad (4.1)$$

This is easy to do, since the longitudinal parts of \vec{G} and \vec{S} can be recovered in the limit $c \rightarrow \infty$,

$$\begin{aligned}\vec{G}_L &\equiv \lim_{c \rightarrow \infty} \vec{G}, \\ \vec{S}_L &\equiv \lim_{c \rightarrow \infty} \vec{S}.\end{aligned}\quad (4.2)$$

We will not write down \vec{G}_L and \vec{S}_L , but they may be found directly from Eqs. (2.5), (2.20), and (4.2). The contribution to $\vec{E}(\vec{\kappa};z)$ in Eq. (2.19) from the longitudinal part of \vec{S} is [see the discussion after Eq. (2.20)] expected on physical grounds to be that due to an image polarization in the bulk. We can identify this by defining an image polarization \vec{P}_I :

$$\begin{aligned}(\hat{x}\hat{x} + \hat{y}\hat{y}) \cdot \vec{P}_I(x,y,z'') \\ = -\frac{\epsilon-1}{\epsilon+1}(\hat{x}\hat{x} + \hat{y}\hat{y}) \cdot \vec{P}(x,y,z'),\end{aligned}\quad (4.3)$$

$$\hat{z}\hat{z} \cdot \vec{P}_I(x,y,z'') = \frac{\epsilon-1}{\epsilon+1} \hat{z}\hat{z} \cdot \vec{P}(x,y,z'),$$

where $0 < z' \leq l$ and $z'' = -z'$; Fourier transforming Eq. (4.3) we have [cf. Eq. (2.3)]

$$\begin{aligned}(\hat{s}\hat{s} + \hat{\kappa}\hat{\kappa}) \cdot \vec{P}_I(\vec{\kappa};z'') \\ = -\frac{\epsilon-1}{\epsilon+1}(\hat{s}\hat{s} + \hat{\kappa}\hat{\kappa}) \cdot \vec{P}(\vec{\kappa};z'),\end{aligned}\quad (4.4)$$

$$\hat{z}\hat{z} \cdot \vec{P}_I(\vec{\kappa};z'') = \frac{\epsilon-1}{\epsilon+1} \hat{z}\hat{z} \cdot \vec{P}(\vec{\kappa};z'),$$

and using Eqs. (2.19) and (4.2)–(4.4) we find

$$\begin{aligned}\int_0^l \vec{S}_L(z+z') \cdot \vec{P}(\vec{\kappa};z') dz' \\ = \int_{-l}^0 \vec{G}_L(z-z'') \cdot \vec{P}_I(\vec{\kappa};z'') dz'',\end{aligned}\quad (4.5)$$

as physically expected. Defining an effective polarization to include the selvedge and image polarizations,

$$\vec{P}_s(\vec{\kappa};z) = \begin{cases} \vec{P}(\vec{\kappa};z), & 0 \leq z \leq l \\ 0 & \text{otherwise} \end{cases}\quad (4.6)$$

$$\vec{P}_e(\vec{\kappa};z) = \begin{cases} \vec{P}_s(\vec{\kappa};z), & 0 \leq z \leq l \\ \vec{P}_I(\vec{\kappa};z), & -l \leq z < 0 \\ 0 & \text{otherwise} \end{cases}$$

and writing

$$\vec{G}'_T(z,z') \equiv \vec{G}_T(z-z') + \vec{S}_T(z+z'),\quad (4.7)$$

Eq. (2.19) becomes

$$\vec{E}(\vec{\kappa};z) = \vec{E}'_i(\vec{\kappa};z) + \int \vec{G}_L(z-z') \cdot \vec{P}_e(\vec{\kappa};z') dz',\quad (4.8)$$

where

$$\vec{E}'_i(\vec{\kappa};z) = \vec{E}_i(\vec{\kappa};z) + \int_0^l \vec{G}'_T(z,z') \cdot \vec{P}(\vec{\kappa};z') dz' \quad (4.9)$$

now contains the complete transverse field to which the selvedge is subject. Expressions for the longitudinal part of the field from a polarization $\vec{P}(\vec{r})$ are well known²⁹; transforming Eq. (4.8) back to real space we find

$$\begin{aligned}\vec{E}(\vec{r}) = \vec{E}'_i(\vec{r}) + \int_{a(|\vec{r}-\vec{r}'|)} \vec{T}(\vec{r}-\vec{r}') \cdot \vec{P}_e(\vec{r}') d\vec{r}' \\ - \frac{4\pi}{3} \vec{P}_e(\vec{r})\end{aligned}\quad (4.10)$$

for points \vec{r} with $z > 0$, where

$$\vec{T}(\vec{r}) = (3\hat{r}\hat{r} - \vec{U})/r^3 \quad (4.11)$$

is the static dipole tensor, \vec{U} being the unit tensor. The notation $a(|\vec{r}-\vec{r}'|)$ indicates that the integral is to be evaluated excluding points \vec{r}' satisfying $|\vec{r}'-\vec{r}| \leq \delta$, and then δ is to be allowed to approach zero. Equations (2.21) and (4.10) determine the polarization in the selvedge.

Equation (4.10) separates the longitudinal, short-range part of the dipole-dipole interaction from the

transverse, long-range part. Let us suppose that Eqs. (2.21) and (4.10) could be solved for $\vec{P}(\vec{r})$ in terms of $\vec{E}_i(\vec{r})$,

$$\vec{P}(\vec{r}) = \int \vec{T}(\vec{r}, \vec{r}') \cdot \vec{E}_i(\vec{r}') d\vec{r}' . \quad (4.12)$$

We would *still* have to solve for $\vec{P}(\vec{r})$ self-consistently, since $\vec{E}_i(\vec{r})$ involves $\vec{P}(\vec{r})$ [Eq. (4.9)]. However, it is easy to verify that $\vec{G}'_T(z, z') \sim \omega'$ in the limit (3.12). Further, since the appropriate dimensionless parameter in \vec{G} and \vec{S} is $c\kappa/\omega = \kappa/\tilde{\omega}$, the limits $c \rightarrow \infty$ and $\kappa \rightarrow \infty$ are the same, and [see Eqs. (4.1) and (4.7)] $\vec{G}'_T(z, z') \rightarrow 0$ for $\kappa \rightarrow \infty$. Thus we can expect, from these limits and Eq. (4.9), that

$$\vec{E}_i(\vec{r}) \lesssim \vec{E}_i(\vec{r}) + O(\tilde{\omega}l)\vec{P}(\vec{r}) . \quad (4.13)$$

$$\vec{P}(\vec{r}) = \chi(\vec{r}) \left[\vec{E}_i(\vec{r}) + \int_{a(|\vec{r}-\vec{r}'|)} \vec{T}(\vec{r}-\vec{r}') \cdot \vec{P}_e(\vec{r}') d\vec{r}' - \frac{4\pi}{3} \vec{P}_e(\vec{r}) \right] \quad (4.14)$$

for points \vec{r} with $z > 0$; introducing an image dipole tensor \vec{T}_I ,

$$\vec{T}_I(\vec{\rho}, z) = -\frac{\epsilon-1}{\epsilon+1} \frac{3\vec{\rho}\vec{\rho} + 2(\rho^2 - z^2)\hat{z}\hat{z} + 3z\hat{z}\vec{\rho} - \vec{U}(\rho^2 + z^2)}{(\rho^2 + z^2)^{5/2}} , \quad (4.15)$$

we may write Eq. (4.14) in terms of the selvedge polarization $\vec{P}_s(\vec{r})$ only,

$$\vec{P}_s(\vec{r}) = \chi(\vec{r}) \left[\vec{E}_i(\vec{r}) + \int_{a(|\vec{r}-\vec{r}'|)} \vec{T}(\vec{r}-\vec{r}') \cdot \vec{P}_s(\vec{r}') d\vec{r}' - \frac{4\pi}{3} \vec{P}_s(\vec{r}) + \int \vec{T}_I(\vec{\rho}-\vec{\rho}'; z+z') \cdot \vec{P}_s(\vec{r}') d\vec{r}' \right] . \quad (4.16)$$

It is also convenient to change the shape of the excluded volume in the integral involving \vec{T} ; as that shape changes, the additional term $-4\pi\vec{P}_s(\vec{r})/3$ must change accordingly to yield the same total longitudinal field (29). If we change the excluded volume to a cylinder with its axis parallel to \hat{z} , and with a height to radius ratio of 2ξ , it is easy to show that

$$\int_{a(|\vec{r}-\vec{r}'|)} \vec{T}(\vec{r}-\vec{r}') \cdot \vec{P}_s(\vec{r}') d\vec{r}' = \int_{\alpha(\vec{r}-\vec{r}')} \vec{T}(\vec{r}-\vec{r}') \cdot \vec{P}_s(\vec{r}') d\vec{r}' + 4\pi \left[\frac{1}{3} - \xi(1+\xi^2)^{-1/2} \right] \vec{P}_s(\vec{r}) - 4\pi\hat{z}\hat{z} \cdot \vec{P}_s(\vec{r}) , \quad (4.17)$$

where $\alpha(\vec{r}-\vec{r}')$ denotes this new excluded volume. Equation (4.17) is found simply by integrating the dipole field from the volume between the sphere and the cylinder; since both excluded volumes are infinitesimal in the limit of interest, $\vec{P}_s(\vec{r})$ can be assumed uniform over the "difference volume." If we now take the limit $\xi \rightarrow 0$ we obtain an infinitesimally thin slab parallel to the xy plane as the excluded volume, and $\alpha(\vec{r}-\vec{r}') \rightarrow a(|z-z'|)$; combining Eqs. (4.16) and (4.17) in this limit we have, for points \vec{r} with $z > 0$,

$$\vec{P}_s(\vec{r}) = \vec{\beta}(\vec{r}) \cdot \left[\vec{E}_i(\vec{r}) + \int_{a(|z-z'|)} \vec{T}(\vec{r}-\vec{r}') \cdot \vec{P}_s(\vec{r}') d\vec{r}' + \int \vec{T}_I(\vec{\rho}-\vec{\rho}'; z+z') \cdot \vec{P}_s(\vec{r}') d\vec{r}' \right] , \quad (4.18)$$

where

$$\vec{\beta}(\vec{r}) = \vec{\beta} b(\vec{r}), \quad \vec{\beta} = \hat{z}\hat{z}(\epsilon-1)/(4\pi\epsilon) + (\hat{x}\hat{x} + \hat{y}\hat{y})(\epsilon-1)/4\pi . \quad (4.19)$$

Since

$$\vec{T}_I(\vec{\rho}; z) \cdot \vec{V} = \vec{V} \cdot \vec{T}_I(-\vec{\rho}, z), \quad \vec{T}(\vec{r}) \cdot \vec{V} = \vec{V} \cdot \vec{T}(-\vec{r}) , \quad (4.20)$$

for any vector \vec{V} , it is easy to verify that Eq. (4.18) may be derived from the variational principle $\delta U = 0$, where

For $\tilde{\omega}l \ll 1$, we neglect the second term on the right-hand side of Eq. (4.13); a more exact treatment would take it into account in a perturbation approach involving the small expansion parameter ($\tilde{\omega}l$). Such a development, which could be pursued using the formal approach of, for example, Bedeaux and Mazur,³⁰ would be in a sense a true "multiple-scattering" expansion, since only the transverse field would be treated iteratively; the longitudinal field would be included exactly, or at least as exactly as the solution (4.12) could be found.

Neglecting multiple-scattering corrections in this sense, we combine Eqs. (2.21) and (4.10) and seek a solution of the approximate equation

$$\begin{aligned}
U = & -\frac{1}{2} \int \vec{P}_s(\vec{r}) \cdot \vec{\beta}^{-1} \cdot \vec{P}_s(\vec{r}) d\vec{r} - \int \vec{P}_s(\vec{r}) \cdot \vec{E}_i(\vec{r}) d\vec{r} - \frac{1}{2} \int_{a(|z-z'|)} \vec{P}_s(\vec{r}) \cdot \vec{T}(\vec{r}-\vec{r}') \cdot \vec{P}_s(\vec{r}') d\vec{r} d\vec{r}' \\
& - \frac{1}{2} \int \vec{P}_s(\vec{r}) \cdot \vec{T}_I(\vec{\rho}-\vec{\rho}'; z+z') \cdot \vec{P}_s(\vec{r}') d\vec{r} d\vec{r}', \quad (4.21)
\end{aligned}$$

and where the integrals in Eq. (4.21) are to range only over the points for which $b(\vec{r}), b(\vec{r}') = 1$.

Ideally, for a given $b(\vec{r})$ one would solve Eq. (4.18), numerically if necessary, for $\vec{P}_s(\vec{r})$. Here we shall merely use the variational principle to construct an approximate solution which, however, takes into account the "shape" of the surface roughness. We first note that, except for its variation in the xy plane, $\vec{E}_i(\vec{r})$ may be taken as uniform over the selvedge [see Eq. (2.20)] in the approximations (3.12). We then assume a selvedge polarization of the form

$$\vec{P}_s(\vec{r}) = \vec{p} b(\vec{r}) \quad (4.22)$$

for points in the selvedge, where \vec{p} is a vector, yet to be determined, that "adiabatically" follows the variation of $\vec{E}_i(\vec{\rho})$ in the xy plane. Putting Eq. (4.22) in Eq. (4.21), we can then extend the integration to all points in the selvedge; we find the best value of \vec{p} overall by minimizing the ensemble average of the resulting expression,

$$\begin{aligned}
U' = & \left(\frac{1}{2} \vec{p} \cdot \vec{\beta}^{-1} \cdot \vec{p} - \vec{p} \cdot \vec{E}_i \right) \int \langle b(\vec{r}) \rangle d\vec{r} - \frac{1}{2} \int_{a(|z-z'|)} \vec{p} \cdot \vec{T}(\vec{r}-\vec{r}') \cdot \vec{p} \langle b(\vec{r}) b(\vec{r}') \rangle d\vec{r} d\vec{r}' \\
& - \frac{1}{2} \int \vec{p} \cdot \vec{T}_I(\vec{\rho}-\vec{\rho}'; z+z') \cdot \vec{p} \langle b(\vec{r}) b(\vec{r}') \rangle d\vec{r} d\vec{r}', \quad (4.23)
\end{aligned}$$

where the angular brackets denote an ensemble average. In writing Eq. (4.23) we have neglected the variation of \vec{E}_i and that of \vec{p} in the xy plane; we will see that, in cases where the variation should be taken into account in the $\langle b(\vec{r}) b(\vec{r}') \rangle$ terms in Eq. (4.23), the contribution from those terms is negligible.

To model the surface roughness, we adopt the simple picture shown in Fig. 5 and put

$$b(\vec{r}) = b(\vec{\rho}). \quad (4.24)$$

Defining the filling factor $F = \langle b(\vec{\rho}) \rangle$, we note that $\langle b(\vec{\rho}) b(\vec{\rho}') \rangle \rightarrow F$ as $|\vec{\rho}' - \vec{\rho}| \rightarrow \infty$ while, assuming the roughness is uncorrelated at large distances, we have $\langle b(\vec{\rho}) b(\vec{\rho}') \rangle \rightarrow F^2$ as $|\vec{\rho}' - \vec{\rho}| \rightarrow 0$. Thus we write

$$\langle b(\vec{\rho}) b(\vec{\rho}') \rangle = F^2 + (F - F^2) C(|\vec{\rho} - \vec{\rho}'|), \quad (4.25)$$

where

$$C(\rho) \rightarrow \begin{cases} 1 & \text{as } \rho \rightarrow 0 \\ 0 & \text{as } \rho \rightarrow \infty. \end{cases} \quad (4.26)$$

Although a Gaussian function might be a more ideal model, we use

$$C(\rho) = \Theta(l_t - \rho) \quad (4.27)$$

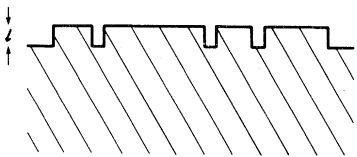


FIG. 5. A simple model of the surface roughness.

instead, where l_t is a transverse correlation length, to make the calculations tractable. Putting Eqs. (4.24)–(4.27) in Eq. (4.23) and setting $\partial U' / \partial \vec{p} = 0$, we find

$$\vec{p} = \gamma_z \hat{z} \hat{z} \cdot \vec{E}_i + \gamma_t (\hat{x} \hat{x} + \hat{y} \hat{y}) \cdot \vec{E}_i, \quad (4.28)$$

where

$$\begin{aligned}
4\pi\gamma_z = & (\epsilon - 1) \{ \epsilon - (1 - F)(\epsilon - 1) \\
& \times [h(s) + R h_I(s)] \}^{-1}, \\
4\pi\gamma_t = & (\epsilon - 1) \left\{ 1 + \frac{1}{2} (1 - F)(\epsilon - 1) \right. \\
& \left. \times [h(s) - R h_I(s)] \right\}^{-1}. \quad (4.29)
\end{aligned}$$

Here we have defined a shape factor $s \equiv l_t / l$ and set $R = (\epsilon - 1) / (\epsilon + 1)$, while

$$\begin{aligned}
h(s) = & (s^2 + 1)^{1/2} - s, \\
h_I(s) = & \frac{1}{2} [(s^2 + 4)^{1/2} + s] - (s^2 + 1)^{1/2}, \quad (4.30)
\end{aligned}$$

the term involving $h_I(s)$ coming from the image integral involving \vec{T}_I in Eq. (4.23), the $h(s)$ term coming from the integral involving \vec{T} .

Although a host of approximations have gone into deriving Eq. (4.28), that equation does at least qualitatively capture the dependence of the effective susceptibilities γ_z and γ_t on the shape and filling factors of the selvedge. Consider first the limit $s \rightarrow \infty$ (slab or "pancake" shape). We find

$$\gamma_z \rightarrow (\epsilon - 1) / (4\pi\epsilon), \quad \gamma_t \rightarrow (\epsilon - 1) / 4\pi, \quad (4.31)$$

as expected for a dielectric slab parallel to the xy plane; in fact, these values are nearly reached for

$s = l_t/l \geq$ only about 10. Since we have assumed $\kappa l \gg 1$ [Eq. (3.12)], this limit is reached long before variations in $\vec{E}_i(\vec{\rho})$ are important over the range of $C(\rho)$; as the result (4.31) can be derived from Eq. (4.23) with the neglect of the last two integrals in that equation, this justifies the statement made after Eq. (4.23). We also find Eq. (4.31) in the limit $F \rightarrow 1$, regardless of the value of s , as expected; in this limit we approach a "full" selvedge. However, for $F \neq 1$, γ_z and γ_t are strong functions of s , especially for large ϵ , as "depolarization effects" become important. While for $s \rightarrow \infty$ we have $\gamma_z \ll \gamma_t$, for $s \rightarrow 0$ (spike or "banana" shape) we find

$$\begin{aligned} \gamma_z &\rightarrow (\epsilon - 1)/4\pi, \\ \gamma_t &\rightarrow (\epsilon - 1)/2\pi(\epsilon + 1), \end{aligned} \quad (4.32)$$

for $F \simeq 0$, and here $\gamma_z \gg \gamma_t$. If we neglect the image contribution by setting $h_I = 0$ in Eq. (4.29), in the limit $F = 0$ we find

$$\gamma_z = \gamma_t = 3(\epsilon - 1)/4\pi(\epsilon + 2), \quad (4.33)$$

the effective susceptibilities for an isolated sphere,³¹ for the not unreasonable value of $s = \frac{5}{12}$. In Fig. 6 we graph the full γ_z and γ_t [Eq. (4.29)] as a function of s , for $F \simeq 0$, taking $\epsilon = 16$. The large variation of γ_z/γ_t will be important in Sec. V, where we will see that the type of fringes created depends critically on that ratio.

We conclude this section by noting that the usual theories of the scattering of light by randomly rough surfaces¹⁶⁻²⁰ give, in their first order, results equivalent to Eqs. (4.28) and (4.31); that is, they implicitly assume $s \gg 1$. In those theories, both the "depolarization" corrections and "true multiple scattering" that result from correlations in $b(\vec{r})$ are taken into account in the same iteration procedure, since the electric field is not split into longitudinal and transverse parts. Thus an infinite number of iterations would be required to obtain the correct qualitative ratio γ_z/γ_t for $s \simeq 1$. Our approach allows us to neglect the indeed small radiative correc-

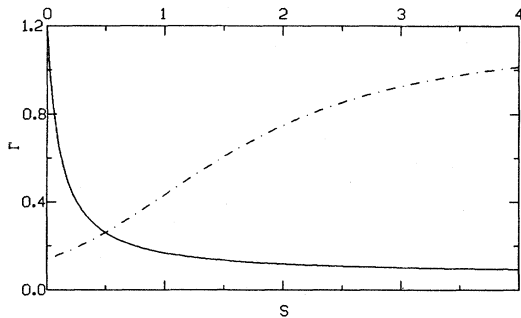


FIG. 6. Effective susceptibilities γ_z (solid line) and γ_t (dash-dots) as a function of s for $F \simeq 0$, $\epsilon = 16$.

tions of Eq. (4.13) while recovering the important depolarization corrections immediately, if only approximately. Of course, our result [(4.22) and (4.28)] could be used as the initial approximation in Eq. (4.18) to lead iteratively to an even better approximate solution.

V. ENERGY DEPOSITION

We can now look at the inhomogeneous energy deposition just below the selvedge. Combining Eqs. (4.22), (4.24), and (4.28), we find

$$\vec{P}(\vec{\rho}) = b(\vec{\rho}) \vec{\gamma} \cdot \vec{E}_i(\vec{\rho}), \quad (5.1)$$

where

$$\vec{\gamma} = \gamma_z \hat{z}\hat{z} + \gamma_t (\hat{x}\hat{x} + \hat{y}\hat{y}) \quad (5.2)$$

and

$$\vec{E}_i(\vec{\rho}) = \vec{E}_i e^{i \vec{\kappa}_i \cdot \vec{\rho}}. \quad (5.3)$$

Here $\vec{\kappa}_i$ is the component of the incident wave vector parallel to the surface and

$$\vec{E}_i = [\vec{U} + \vec{r}(\vec{\kappa}_i)] \cdot \vec{E}_0 \quad (5.4)$$

follows from Eq. (2.20), where we have used the approximations (3.12) and assumed an incident infinite plane wave for simplicity. For the moment we look at just one Fourier component of the roughness function $b(\vec{\kappa})$ and put

$$b(\vec{\rho}) = b(\vec{\kappa}) e^{i \vec{\kappa} \cdot \vec{\rho}} + b^*(\vec{\kappa}) e^{-i \vec{\kappa} \cdot \vec{\rho}} \quad (5.5)$$

in Eq. (5.1), with Eq. (5.3), to obtain

$$\vec{Q}(\vec{\rho}) = \vec{Q}_+ e^{i \vec{\kappa}_+ \cdot \vec{\rho}} + \vec{Q}_- e^{i \vec{\kappa}_- \cdot \vec{\rho}} \quad (5.6)$$

from Eq. (3.13) where $\vec{\kappa}_\pm = \vec{\kappa}_i \pm \vec{\kappa}$ and

$$\begin{aligned} \vec{Q}_+ &= b(\vec{\kappa}) l \vec{\gamma} \cdot \vec{E}_i, \\ \vec{Q}_- &= b^*(\vec{\kappa}) l \vec{\gamma} \cdot \vec{E}_i. \end{aligned} \quad (5.7)$$

From Eqs. (2.9), (2.11), and (5.6) we can now find the electric field in the bulk,

$$\vec{E}(\vec{r}) = \vec{E}^{(0)}(\vec{r}) + \vec{E}^{(1)}(\vec{r}), \quad (5.8)$$

where

$$\begin{aligned} \vec{E}^{(0)}(\vec{r}) &= \vec{t}(\vec{\kappa}_i) \cdot \vec{E}_0 e^{i \vec{\kappa}_i \cdot \vec{\rho}} e^{-i \omega(\vec{\kappa}_i)z} \\ &\equiv \vec{E}_t e^{i \vec{\kappa}_i \cdot \vec{\rho}} e^{-i \omega(\vec{\kappa}_i)z} \end{aligned} \quad (5.9)$$

is the refracted field that would be present without the selvedge, and

$$\begin{aligned} \vec{E}^{(1)}(\vec{r}) &= \vec{E}_+ e^{i \vec{\kappa}_+ \cdot \vec{\rho}} e^{-i \omega(\vec{\kappa}_+)z} \\ &\quad + \vec{E}_- e^{i \vec{\kappa}_- \cdot \vec{\rho}} e^{i \omega(\vec{\kappa}_-)z} \end{aligned} \quad (5.10)$$

is the field from the selvedge, where

$$\begin{aligned}\vec{E}_{\pm} &= \vec{t}(\vec{\kappa}_{\pm}) \cdot \vec{g}_{\pm}(\vec{\kappa}_{\pm}) \cdot \vec{Q}_{\pm} \\ &\equiv 2\pi\tilde{\omega} \vec{h}(\vec{\kappa}_{\pm}) \cdot \vec{Q}_{\pm}.\end{aligned}\quad (5.11)$$

Now the energy absorbed in the bulk is proportional to $A(\vec{r}) \equiv |\vec{E}(\vec{r})|^2$, and assuming the field from the selvedge is a small perturbation we take $|\vec{E}^{(1)}| \ll |\vec{E}^{(0)}|$ and find

$$A(\vec{r}) \simeq 2 \operatorname{Re}[\vec{E}^{(0)*}(\vec{r}) \cdot \vec{E}^{(1)}(\vec{r})] \quad (5.12)$$

for the inhomogeneous part of $A(\vec{r})$. At $z=0$ —this reduces to

$$\begin{aligned}A(\vec{\rho}) &= 4\pi\tilde{\omega}l \operatorname{Re}\{b(\vec{\kappa})[\nu(\vec{\kappa}_+) + \nu^*(\vec{\kappa}_-)] \\ &\quad \times e^{i\vec{\kappa} \cdot \vec{\rho}}\},\end{aligned}\quad (5.13)$$

where we have set

$$\nu(\vec{\kappa}_{\pm}) \equiv \vec{E}_t^* \cdot \vec{h}(\vec{\kappa}_{\pm}) \cdot \vec{\gamma} \cdot \vec{E}_i. \quad (5.14)$$

Clearly the magnitude of $A(\vec{\rho})$ in Eq. (5.13) is proportional to $|b(\vec{\kappa})[\nu(\vec{\kappa}_+) + \nu^*(\vec{\kappa}_-)]|$; for a sum of Fourier components of roughness we will obviously obtain

$$A(\vec{\kappa}) \propto \eta(\vec{\kappa}; \vec{\kappa}_i) |b(\vec{\kappa})|, \quad (5.15)$$

where the efficacy factor for the inhomogeneous energy deposition at $\vec{\kappa}$, due to an incident beam characterized by $\vec{\kappa}_i$, is given by

$$\eta(\vec{\kappa}; \vec{\kappa}_i) = 2\pi |\nu(\vec{\kappa}_+) + \nu^*(\vec{\kappa}_-)|. \quad (5.16)$$

Recalling our simple model that predicts large damage wherever $A(\vec{\rho})$ is large, we recover the prediction (1.1) for the intensity of the diffracted probe radiation. We note that, because $b(\vec{\rho})$ is a real function [Eq. (5.5)], we have $I(\vec{\kappa}) = I(-\vec{\kappa})$.

To find the dependence of $\eta(\vec{\kappa}; \vec{\kappa}_i)$ on $\vec{\kappa}$, we note first that Eq. (5.11) gives

$$\vec{h}(\vec{\kappa}) = \sum_{i,j} h_{ij} \hat{e}_i \hat{e}_j, \quad (5.17)$$

where $\hat{e}_i = \hat{s}, \hat{\kappa},$ and \hat{z} , and

$$\begin{aligned}h_{ss} &= 2i\tilde{\omega}(w_0 + w)^{-1}, \\ h_{\kappa\kappa} &= 2iw_0\tilde{\omega}^{-1}(w_0\epsilon + w)^{-1}, \\ h_{zz} &= 2i\kappa^2\tilde{\omega}^{-1}(w_0\epsilon + w)^{-1}, \\ h_{z\kappa} &= 2i\kappa w_0\tilde{\omega}^{-1}(w_0\epsilon + w)^{-1}, \\ h_{\kappa z} &= 2iw_0\tilde{\omega}^{-1}(w_0\epsilon + w)^{-1},\end{aligned}\quad (5.18)$$

with all other h_{ij} vanishing. These functions are similar to the f 's of Sec. III; since $\vec{h}(\vec{\kappa}_{\pm})$ appear in $\eta(\vec{\kappa}; \vec{\kappa}_i)$, we can expect “kinks” (and perhaps peaks; cf. Figs. 2–4) in $\eta(\vec{\kappa}; \vec{\kappa}_i)$ at values of $\vec{\kappa}$ satisfying one or both of Eqs. (1.2), signaling the generation of

radiation remnants. However, the situation is complicated by the fact that $\vec{h}(\vec{\kappa}_+)$ and $\vec{h}(\vec{\kappa}_-)$ must be added “in phase” [Eq. (5.14)], corresponding to sum and difference combinations between the incident $\vec{\kappa}_i$ and the surface roughness $\vec{\kappa}$ [Eq. (5.10)], and by the fact that the h_{ij} will appear with different factors due to different angles between $\vec{\kappa}$ and the appropriate polarization components in the selvedge. Further, for p -polarized light, γ_z and γ_t will appear with factors that vary with the angle of incidence.

The final expression for $\nu(\vec{\kappa}_{\pm})$ is found to be

$$\begin{aligned}\nu(\vec{\kappa}_{\pm}) &= [h_{ss}(\kappa_{\pm})(\hat{\kappa}_{\pm} \cdot \hat{x})^2 + h_{\kappa\kappa}(\kappa_{\pm})(\hat{\kappa}_{\pm} \cdot \hat{y})^2] \\ &\quad \times \gamma_t |t_s(\vec{\kappa}_i)|^2\end{aligned}\quad (5.19)$$

for s -polarized light, where we take $\vec{\kappa}_i$ in the \hat{x} direction. For p -polarized light we find the more complicated expression

$$\begin{aligned}\nu(\vec{\kappa}_{\pm}) &= [h_{ss}(\kappa_{\pm})(\hat{\kappa}_{\pm} \cdot \hat{y})^2 + h_{\kappa\kappa}(\kappa_{\pm})(\hat{\kappa}_{\pm} \cdot \hat{x})^2] \\ &\quad \times \gamma_t |t_x|^2 + h_{\kappa z}(\kappa_{\pm})(\hat{\kappa}_{\pm} \cdot \hat{x})\gamma_z \epsilon t_x^* t_z \\ &\quad + h_{z\kappa}(\kappa_{\pm})(\hat{\kappa}_{\pm} \cdot \hat{x})\gamma_t t_z^* t_x \\ &\quad + h_{zz}(\kappa_{\pm})\gamma_z \epsilon |t_z|^2,\end{aligned}\quad (5.20)$$

where t_x and t_z

$$\begin{aligned}t_x &= w(\kappa_i)(\tilde{\omega}n)^{-1}t_p(\kappa_i), \\ t_z &= \kappa_i(\tilde{\omega}n)^{-1}t_p(\kappa_i),\end{aligned}\quad (5.21)$$

give the amplitude of the x and z components of the refracted beams; in Eqs. (5.20) and (5.22) we have set $|\vec{E}_0| = 1$.

Because of the complicated form of the efficacy factor $\eta(\vec{\kappa}; \vec{\kappa}_i)$, we defer a detailed discussion of its dependence on $\vec{\kappa}$ and $\vec{\kappa}_i$ to a comparison of theory and experiment.²⁴ We here present only a few comments on the general form of η . First we note that, although for p -polarized light η depends on the ratio γ_z/γ_t , and thus on the roughness parameters s and F of the selvedge, for s -polarized light η is independent of that ratio. Therefore, although for s -polarized light the overall magnitude of the predicted $I(\vec{\kappa})$ depends on s and F , the $\vec{\kappa}$ dependence of that function does not, except insofar as the $\vec{\kappa}$ dependence of $|b(\vec{\kappa})|$ is important. To a good approximation, then, if $|b(\vec{\kappa})|$ is indeed a slowly varying function, the predicted $I(\vec{\kappa})$ for s -polarized light is independent of any adjustable parameters that might be used to model an imperfectly known surface roughness spectrum. The comparison of our predicted results with the experimental results for s -polarized light thus will yield a critical test of our simple picture for damage formation.

A second point is that, although the values of $f_s(\kappa)$ at $\kappa = \tilde{\omega}$ and $\tilde{\omega}n$ are equal, and in fact the con-

tribution from $\kappa \approx \tilde{\omega}n$ is more important in the asymptotic expansion (3.22), this does not hold for $f_\kappa(\kappa)$ and $f_z(\kappa)$. In those functions a much stronger magnitude appears at $\kappa \approx \tilde{\omega}$ than at $\kappa \approx \tilde{\omega}n$, as seen from Figs. 3 and 4. As we noted in Sec. III, the asymptotic expansions indicate this is because we chose $n \gg 1$ and indeed calculations of $f_\kappa(\kappa)$ and $f_z(\kappa)$ for $n \geq 1$ give much larger relative contributions from the neighborhood of $\kappa \approx \tilde{\omega}n$. Thus, on the whole, we can expect condition (1.2b) to apply only for dielectrics with such values of n . In detail, however, the situation is fairly complicated: For $n \approx 1.5$, for example, the imaginary part of $f_\kappa(\kappa)$ in fact exhibits a peak at $\kappa \approx 1.25\tilde{\omega}$. We plan to turn to the problem of damage in low-index dielectrics in a future publication.

Finally, we consider the problem of damage at metal surfaces, where at frequencies corresponding to visible and infrared light the real part of ϵ is large and negative. Here we find that $f_s(\kappa) = h_{ss}(\kappa)$ exhibit small kinks at $\kappa \approx \tilde{\omega}$; but $f_\kappa(\kappa)$, $f_z(\kappa)$, and the other h_{ij} of Eq. (5.18) show a sharp resonant structure due to the excitation of surface plasmons: $(w_0\epsilon + w)^{-1}$ diverges at the (complex) surface-plasmon wave number, given by³²

$$\kappa = \tilde{\omega}[\epsilon/(\epsilon + 1)]^{1/2}. \quad (5.22)$$

In Fig. 7 we show $f_\kappa(\kappa)$ for an underlying bulk with $n = 1.8 + i9.3$, the value³³ for Al at $\lambda \approx 1.06 \mu\text{m}$. Since, for $|\epsilon| \gg 1$, Eq. (5.22) gives $\kappa \approx \tilde{\omega}$, we can expect that metals, as well as materials with large and positive ϵ , will show damage structure following condition (1.2a), although the details will, of course, be different.

VI. SUMMARY

We close by summarizing our results: We have developed a theory for the periodic damage patterns produced by laser irradiation near the damage threshold, based on the assumption that the damage patterns result from inhomogeneous energy absorp-

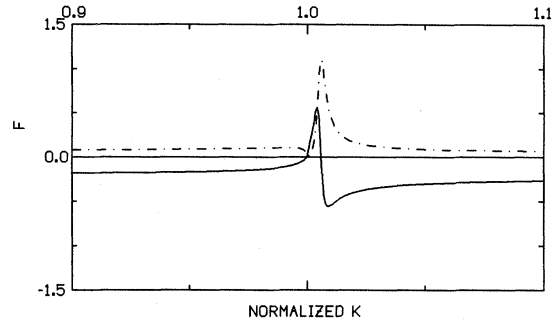


FIG. 7. $-\text{Re}f_\kappa(\kappa)$ (solid line) and $\text{Im}f_\kappa(\kappa)$ (dash-dots) for an underlying bulk with $\epsilon = n^2$, $n = 1.8 + i9.3$.

tion just beneath the surface, induced by surface roughness. Our detailed predictions for the damage structure in \vec{k} space, Eqs. (1.1) and (5.16)–(5.21), are, except for overall magnitude, independent of the details of the roughness if the damaging beam is s polarized; this should lead to an unambiguous comparison of theory with experiment. For a damaging beam that is p polarized, we predict a dependence on shape and filling factors of the roughness, a dependence which has been calculated by a new approach to the electrodynamics of randomly rough surfaces based on a separate treatment of the transverse and longitudinal electric fields, including local field effects, by introducing a variational principle to deal with the latter. A cursory examination of our predictions indicates condition (1.2), which includes many fringe spacings and directions observed to date as special cases, should result; we defer a detailed comparison of theory and experiment to the following paper.²⁴

ACKNOWLEDGMENTS

We gratefully acknowledge research support from the Natural Sciences and Engineering Research Council of Canada including the awards of scholarships to J.F.Y. and J.S.P.

¹M. Birnbaum, *J. Appl. Phys.* **36**, 3688 (1965).

²D. C. Emmony, R. P. Howson, and L. J. Willis, *Appl. Phys. Lett.* **23**, 598 (1973).

³H. J. Leamy, G. A. Rozgonyi, T. T. Sheng, and G. K. Celler, *Appl. Phys. Lett.* **32**, 535 (1978).

⁴G. N. Maracas, G. L. Harris, C. A. Lee, and R. A. McFarlane, *Appl. Phys. Lett.* **33**, 453 (1978).

⁵M. Oron and G. Sorensen, *Appl. Phys. Lett.* **35**, 782 (1979).

⁶J. F. Young, J. E. Sipe, M. I. Gallant, J. S. Preston, and H. M. van Driel, in *Laser and Electron Beam Interac-*

tions with Solids, edited by B. R. Appleton and G. K. Celler (North-Holland, Amsterdam, 1982), p. 233.

⁷P. M. Fauchet and A. E. Siegman, *Appl. Phys. Lett.* **40**, 824 (1981).

⁸T. E. Zavecz and M. A. Saifi, *Appl. Phys. Lett.* **26**, 165 (1975).

⁹J. C. Koo and R. E. Slusher, *Appl. Phys. Lett.* **28**, 614 (1976).

¹⁰N. R. Isenor, *Appl. Phys. Lett.* **31**, 148 (1977).

¹¹A. K. Jain, V. N. Kulkarni, D. K. Sood, and J. S. Up-
pal, *J. Appl. Phys.* **52**, 4882 (1981).

- ¹²P. A. Temple and M. J. Soileau, *IEEE J. Quant. Elec.* **QE-17**, 2067 (1981).
- ¹³J. A. van Vechten, *Solid State Commun.* **39**, 1285 (1981).
- ¹⁴N. Bloembergen, *Appl. Opt.* **12**, 661 (1973).
- ¹⁵J. F. Young, J. E. Sipe, J. S. Preston, and H. M. van Driel, *Appl. Phys. Lett.* **41**, 261 (1982).
- ¹⁶E. Kroger and E. Kretschmann, *Z. Phys.* **237**, 1 (1970).
- ¹⁷J. M. Elson and R. H. Ritchie, *Phys. Status Solidi (b)* **62**, 461 (1974).
- ¹⁸A. A. Maradudin and D. L. Mills, *Phys. Rev. B* **11**, 1392 (1975).
- ¹⁹V. Celli, A. Marvin, and F. Toigo, *Phys. Rev. B* **11**, 1779 (1975).
- ²⁰F. Toigo, A. Marvin, V. Celli, and N. R. Hill, *Phys. Rev. B* **15**, 5618 (1977).
- ²¹See, e.g., M. Moskovits, *J. Chem. Phys.* **69**, 4159 (1978).
- ²²See, e.g., M. J. Dignam and M. Moskovits, *J. Chem. Soc. Faraday Trans. 2* **69**, 65 (1973).
- ²³M. Born and E. Wolf, *Principles of Optics*, 3rd ed. (Pergamon, New York, 1965), Sec. 2.4.
- ²⁴J. F. Young, J. S. Preston, H. M. van Driel, and J. E. Sipe, *Phys. Rev. B* **27**, 1155 (1983).
- ²⁵J. E. Sipe, *Surf. Sci.* **84**, 75 (1979).
- ²⁶J. E. Sipe, *Phys. Rev. B* **22**, 1589 (1980).
- ²⁷J. E. Sipe, *Surf. Sci.* **105**, 489 (1981).
- ²⁸After a certain amount of algebra the Fourier integrals in Sec. III can be written as a sum of integrals for which asymptotic expansions can be obtained following A. Erdelyi, *Asymptotic Expansions* (Dover, New York, 1956), Sec. 2.8.
- ²⁹J. Van Kranendonk and J. E. Sipe, *Prog. Opt.* **15**, 247 (1977).
- ³⁰D. Bedeaux and P. Mazur, *Physica (Utrecht)* **67**, 23 (1973).
- ³¹H. C. Van de Hulst, *Light Scattering by Small Particles*, (Wiley, New York, 1957).
- ³²M. Cardona, *Am. J. Phys.* **39**, 1277 (1971).
- ³³*American Institute of Physics Handbook*, 3rd ed., edited by D. E. Gray (McGraw-Hill, New York, 1972), Sec. 6.